two, can be significantly reduced. Even such techniques as depositing the slow wave line directly on the ferrite may be useful. However, techniques for reducing the magnetic losses are not as obvious.

A typical multibit meander line phase shifter design is depicted in Fig. 11.

VI. Conclusions

The characteristcs of the device described offer significant advantages over conventional phase shifters. These advantages include low switching energy and compact size. In particular, this design is suited for phased array applications where printed circuit techniques may be employed. The device may prove even more valuable at lower frequencies (L and S band).

Acknowledgment

The author wishes to thank Dr. L. R. Whicker, F. L. Washburn, and J. A. Kempic for their helpful discussions and suggestions throughout the program.

References

[1] H. A. Hair, "Development of helical phase shifter," General Electric Co., Syracuse N. Y., Final Rept. Subcontract 250, Prime AF19(628)500, December 1964.
[2] R. A. Henschke et al., "Ferrite devices for receiving systems," Melabs., Palo Alto, Calif., Final Rept. Contract DA 36-039 SC 85296, 12 October 1959.
[3] J. C. Cromack, "A wide-tuning range S-band traveling-wave maser," Electronic Lab., Stanford University, Stanford, Calif. Tech. Rept. 155-5, Contract DA-36-039, SC-90839, April 1963.
[4] J. T. Bolljahn and G. L. Matthaei, "Microwave filters and coupling structures," Stanford Research Inst., Menlo Park, Calif., Contract DA-36-039, SC-87398, First Quarterly, March 1961

A Miniaturized C-Band Digital Latching Phase Shifter

J. K. PARKS, B. R. SAVAGE, MEMBER, IEEE, L. J. LAVEDAN, JR., MEMBER, IEEE, AND J. BROWN, JR., MEMBER, IEEE

Abstract—This paper describes a digital-latching phase shifter which combines the electrical advantages of waveguide design with the compactness of a strip transmission-line structure. Two multibit, nonreciprocal, C-band models are described, which combine the electronic drivers and the microwave structure in an 0.8 by 0.8 inch cross section designed specifically for half-wavelength stacking in an antenna array.

A new technique of antisymmetric dielectric loading to convert microwave energy from a TEM mode in stripline transmission to a TE-type mode propagating in a dielectrically loaded rectangular waveguide is presented.

Data for a one-bit model are presented along with an investigation into an optimum material choice. Temperature stability and peak power capability are also discussed.

The performance of two multibit models are presented, including VSWR, insertion loss, and average power characteristics of the final microwave structures. Temperature variation of phase shift and peak power performance of these devices are also presented.

Particular attention is given the electronic drivers for the multibit models which must latch the toroids into their remanent states. The driver circuit is designed to permit switching of each bit between states with a single wire trigger.

Finally, the advantages of this design over previous miniaturized models are summarized, and further investigations into other features for greater optimization are suggested.

Manuscript received May 31, 1966; revised August 8, 1966.
The authors are with the Sperry Microwave Electronics Company, Sperry Rand Corporation, Clearwater, Fla.

Introduction

IN A PHASED array antenna system, beam steering capability is enhanced by locating the radiating elements on half-wavelength ($\lambda_0/2$) centers. If the phase shifters themselves are used as the radiating elements or positioned near the antenna, the cross section of the phase shifters must meet this critical stacking requirement. For instance at 5650 MHz, if maximum beam steering capability is desired, the phasors must be located approximately on one-inch centers.

Recent developments in rectangular waveguide digital phase shifters have been directed primarily toward achieving good electrical performance or half-wavelength stacking in one plane only with miniaturization as a secondary objective [1]. Although these devices represent marked advances over previous ferrite phase shifters which required an external field, only limited effort has been concentrated on designing digital components to meet critical antenna space requirements, and to operate under typical environmental conditions.

TEM Phase Shifters

In the past, efforts to miniaturize digital ferrite phase shifters have centered chiefly on strip transmission line

and coaxial structures [2], [3]. While these designs have demonstrated digital latching performance and some reduction in physical size compared to conventional waveguide phasors, they are generally more frequency sensitive and more susceptible to high peak power effects.

Stripline-Waveguide Hybrid Model

This work describes a phase shifter which combines the desired electrical performance of rectangular waveguide construction with the compactness of coaxial or strip transmission line. The device is made possible by the introduction of a new "in-line" stripline to loaded waveguide transition, which is based on an asymmetric dielectric loading technique. Loading the stripline in an asymmetric fashion with two different dielectrics converts propagation from a TEM to a TE mode. The stripline can then be removed from the ferrite portion of the device and a TE configuration will interact with the ferrimagnetic material.

The space required for the transition device is small since bulky waveguide inputs are unnecessary. Sufficient ferrite loading of the waveguide portion of the device allows propagation in C-band at greatly reduced cross section. The electronic driver circuit, which latches the toroids into the $+4\pi M_r$ and $-4\pi M_r$ remanent states, is positioned adjacent to the microwave structure to form a complete phase shifter having a cross section of 0.8 by 0.8 inch.

Transition Device Design

Figure 1 shows the basic configuration used in the stripline-waveguide hybrid model ferrite phase shifter. The transition device itself is shown in greater detail in Fig. 2.[1] The strip center conductor of a rectangular coaxial transmission line is widened into a septum which splits the microwave structure into two rectangular waveguides through which the upper and lower portions of the wave propagate. A low-loss dielectric block ϵ_1 centrally loads the upper rectangular section and a different dielectric block ϵ_2 centrally loads the lower section. Thin dielectric steps having a dielectric constant ϵ_2 are located above and below the strip center conductor just preceding the divided rectangular structures. Dielectric blocks ϵ_1 and ϵ_2 and the septum are of equal length L and comprise an assembly which abuts the leading toroid of the ferrite portion of the device. The septate structure terminates the strip transmission line, and the ferrite toroids are positioned similarly to those in other nonreciprocal rectangular waveguide phase-shift devices.

Microwave energy enters the 50 ohm stripline portion of the device from a coaxial input and the usual TEM mode is set up on the strip. Since the dielectric steps immediately preceding the blocks are more narrow than the strip center conductor, the wave is distorted and a longitudinal component of RF magnetic field is generated along the interface between the two dissimilar dielectrics (air and ϵ_2). This is analogous to the case of the partially loaded coaxial line in which an axial component of RF magnetic field is similarly generated [4]. Due to the presence of axial components of RF magnetic field in the region of the steps, it is reasonable to assume that the waves which propagate in the rectangular guides above and below the septum will have TE configurations when the dielectric block constants ϵ_1 and ϵ_2 are properly adjusted. Since ϵ_1 is unequal to ϵ_2, the wavelength is different in the top and bottom sections of this "septate" guide and a relative phase shift will take place. Furthermore, when this phase shift is 180 degrees, the two RF voltages add in phase at the output end of the septum, which completes the condition for launching a TE_{10} wave into the ferrite loaded waveguide portion of the structure.

By proper adjustment of the length L of the dielectric blocks, the dielectric constants ϵ_1 and ϵ_2, the dielectric widths C_1 and C_2, and the widths of the two septate guides, a_1 and a_2, it should be possible to maintain a phase shift of 180 degrees within a tolerable error over a 10 percent bandwidth.

From Vartanian et al. [5], the phase constants β_1 and β_2 can be calculated for the upper and lower portions of the septate waveguides, respectively. Setting $(\beta_1-\beta_2)L = \pi$ degrees establishes the criteria for the dimensions of the transition.

For initial calculations, the following parameters were chosen to determine L:

$$a_1 = 0.550 \text{ inch}$$
$$a_2 = 0.530 \text{ inch}$$
$$C_1 = 0.275 \text{ inch}$$
$$C_2 = 0.275 \text{ inch}$$
$$\epsilon_1 = 16$$
$$\epsilon_2 = 9$$

With the use of Reference [5] the following values were determined for L at G-band frequencies:

Freq (GHz)	$\beta_1(\text{in}^{-1})$	$\beta_2(\text{in}^{-1})$	L(in)
5.4	9.25	5.66	0.874
5.65	9.64	6.04	0.872
5.9	10.30	6.60	0.850

Small variations in the chosen parameters change L by only a few percent, since at large C/a ratios the fields are almost completely concentrated in the dielectric blocks ϵ_1 and ϵ_2. To match the impedance of the 50 ohm strip transmission line to that of the garnet loaded waveguide, we require $Z_1+Z_2=Z_g$ and

$$\frac{1}{Z_1}+\frac{1}{Z_2}=\frac{1}{50},$$

[1] Several new "end-fire" stripline to waveguide transitions using asymmetric dielectric loading techniques were developed as a result of this study. The authors are particularly indebted to W. B. Day for his analysis of the early dielectric transitions and the conception and development of the design described in this paper.

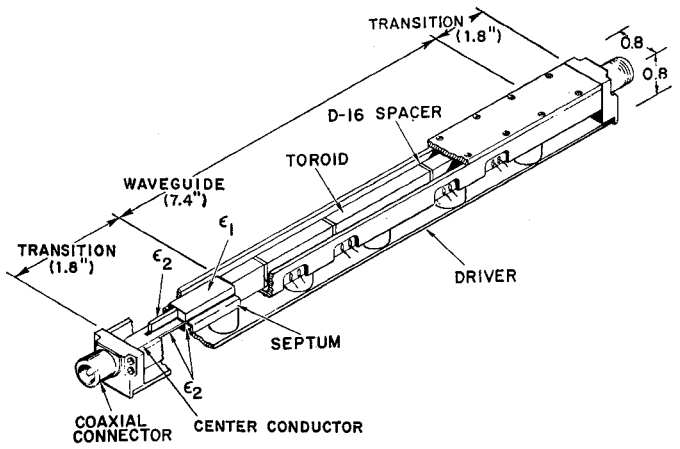

Fig. 1. Stripline transmission-rectangular waveguide phase shifter configuration.

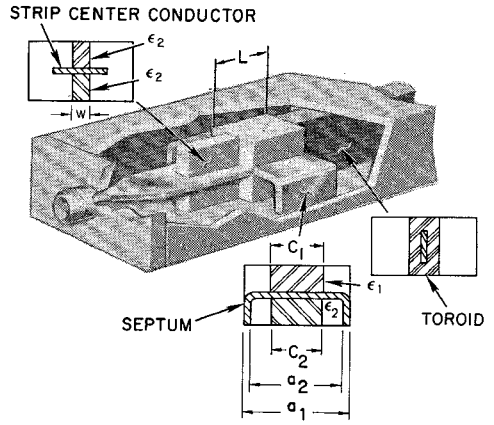

Fig. 2. Stripline to loaded waveguide transition device.

where Z_1 and Z_2 are the power voltage impedances of upper and lower sections of the septate waveguides, and Z_g is the impedance of the garnet loaded structure. However, at a C/a ratio of 0.41 at 5650 MHz, the calculated power voltage impedance of the garnet loaded waveguide ($\epsilon_g = 16$) is 152 ohms. No combination of Z_1 and Z_2 totaling 152 ohms will yield a parallel resistance as high as 50 ohms, and additional matching is required. The addition of the dielectric steps previously discussed above and below the strip center conductor adequately fills this matching requirement. Smith chart techniques were employed to determine the proper size dielectric steps needed for low VSWR. Adjustment of the dielectric step width W and length l gave reasonably good results over a 10 percent bandwidth for $L = 0.850$ inch as shown in Fig. 3.

Since the microwave energy is converted to a TE configuration by the transition structure, propagation through the ferrite portion of the device should be similar to propagation of TE waves through any other rectangular waveguide under similar frequency and loading conditions. The experiments and data discussed below have fully verified this conclusion.

One Bit Test Model Phase Shifter

The phase shift of a test model using a 2.8 inch toroid and the transition structure described above was measured to determine the ferrite loading conditions which would give minimum phase slope. An inside waveguide width of 0.550 inch was chosen as being the largest possible width within the $\lambda_0/2$ requirement and practical mechanical constraints. Zero phase slope was achieved

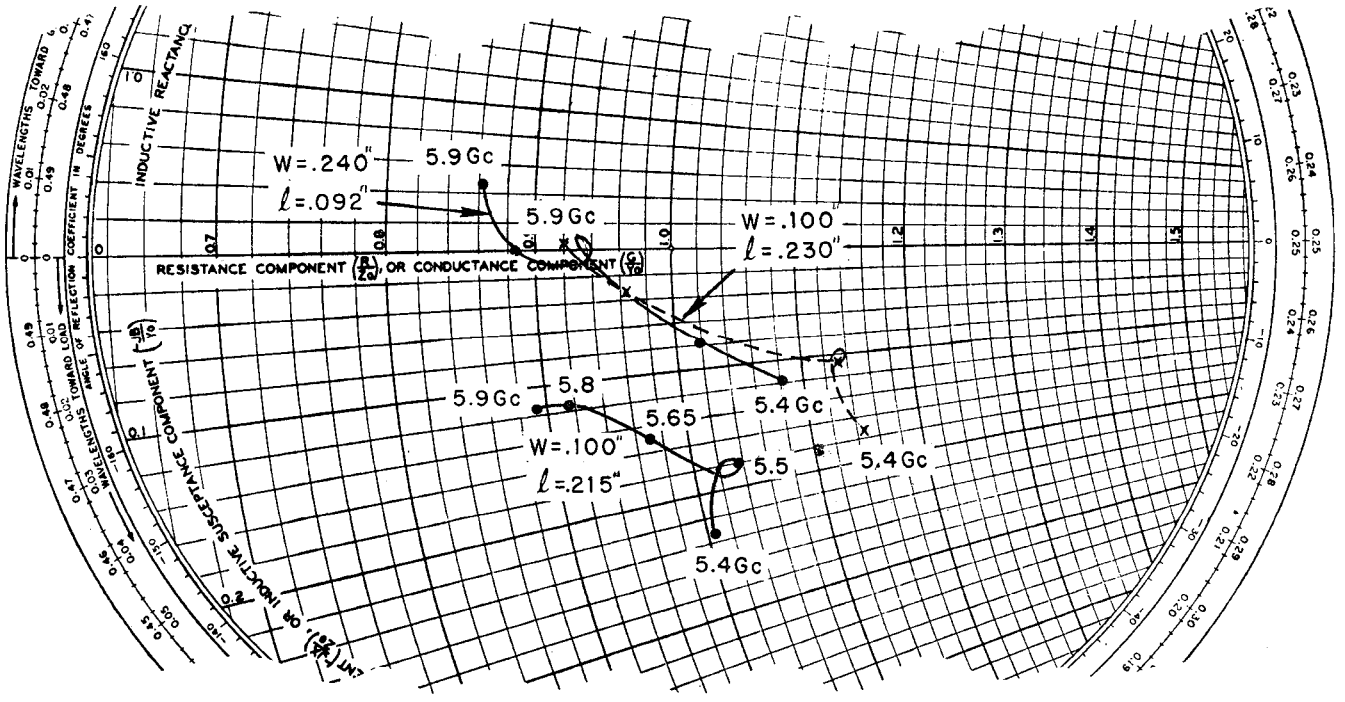

Fig. 3. Effect of varying dielectric step dimensions on transition impedance.

TABLE I
MATERIAL PARAMETERS OF SEVERAL GARNETS TESTED IN ONE-BIT MODEL

Sperry Material Number	Composition	$4\pi M_s$ (gauss)	ω_m	ΔH (Oe)	Dielectric Loss Tangent
G 251	5% Al-15% Gd YIG	1150	0.56	42	0.0005
G 296	30% Gd YIG	1250	0.62	64	0.0006
G 297	45% Gd YIG	1000	0.49	98	0.0008
G 413	45% Gd 1% Dy YIG	1025	0.51	161	0.0008
G 298	60% Gd YIG	750	0.37	177	0.0012

at a toroid width of 0.225 inch using a gadolinium aluminum garnet (Sperry G 251). This toroid to guide width ratio and the measured differential phase shift are in general agreement with other theoretical and empirical investigations into waveguide devices [6], [7]. The quarter-inch waveguide height represents a reduction of 60 percent from normal G-band size and is one of the basic novel features of this design.

The calculated cutoff frequency for the TE_{10} mode in this configuration using a dielectric constant of 16 for the garnet material is approximately 3100 MHz for a toroid width of 0.225 inch [5]. For an empty waveguide with a width of 0.550 inch the calculated cutoff frequency is approximately 10.7 GHz. Thus, the transition device described above provides a method of launching a TE wave directly into a heavily dielectric loaded waveguide in which propagation is restricted to the dominant mode.

Materials from the ferrimagnetic family

$$3[xY_2O_3 \cdot (1 - x)RE] \cdot 5[wFe_2O_3 \cdot (1 - w)Al_2O_3]$$

were investigated in this structure to determine the appropriate ranges of the various material parameters required to yield a device with the following characteristics:

VSWR	1:25:1 max
Loss	1 dB max
Peak Power	5 kW max
Avg Power	250 watts max
Phase Stability	±4 percent from 10°C to 60°C.

The characteristics of some of the materials used in the test model are shown in Table I.

Figure 4 shows the temperature characteristics of the one-bit model using several garnet materials with varying gadolinium content. The addition of gadolinium is seen to increase the stability of the device with ambient temperature. However, the heavily gadolinium doped materials typically are more lossy than those less heavily doped. It is this factor which ultimately limits this percentage to small values. This is especially true in high-power applications where further doping actually is found to decrease phase stability with power because of an increased power-absorption rate.

The insertion loss as a function of peak power of several materials in the one-bit test model is shown in Fig. 5. The peak-power limiting threshold is a strong function of $4\pi M_s$, and depends to a smaller degree upon the linewidth of the material and the geometry of the structure. The typical characteristic of threshold as a function of $4\pi M_s$ for the geometry used is shown in Fig. 6. The parameter ω_m is defined as follows:

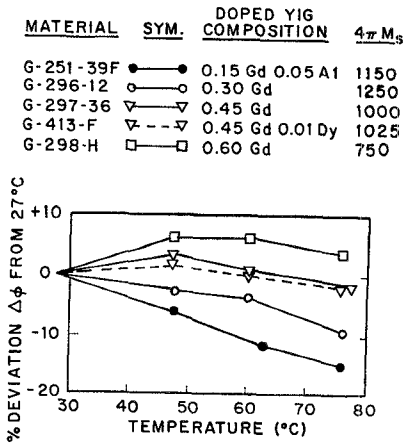

Fig. 4. Phase shift variation with temp.

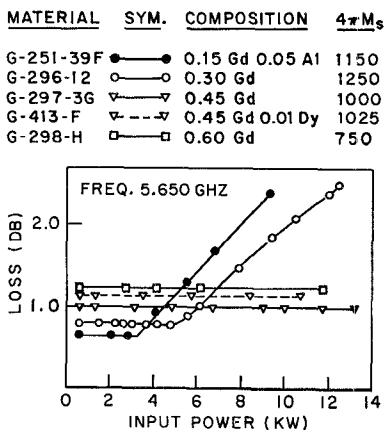

Fig. 5. Peak power data of several garnet materials in the one-bit model.

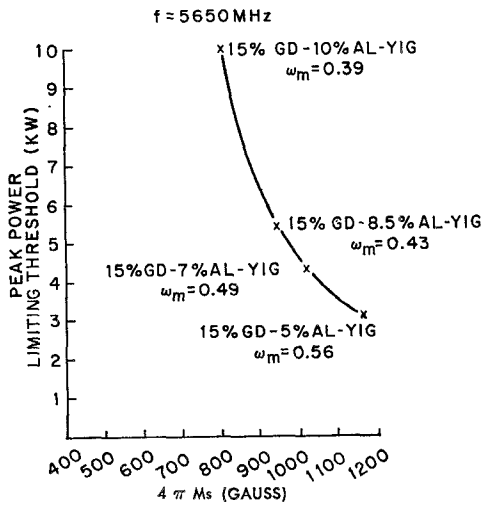

Fig. 6. Peak power threshold vs. $4\pi M_s$ for 15 percent Gd doped YIG.

$\omega_m = (\gamma 4\pi M_s)/f$ = normalized saturation magnetization
$4\pi M_s$ = saturation magnetization of the material (gauss)
γ = gyromagnetic ratio = 2.8 MHz/Oe
f = frequency (MHz).

The four materials utilized in Fig. 6 are of the gadolinium-aluminum family, where the gadolinium is fixed at 15 percent and the aluminum is adjusted to set the desired $4\pi M_s$. The linewidth and geometry are the same for the four examples. At $\omega_m = 0.39$ (G 302 material) the peak-power threshold is approximately 10 kW. This same material in a G-band phase shifter under similar loading conditions yields a peak power threshold of 55 kW, which compares to an h_{crit} value of 47 oersteds [8]. The data shown in Fig. 6 agrees with theoretical investigations into the critical dependence of peak power threshold on ω_m [9].

Multibit Models

Sufficient data was taken on the one-bit test model to select materials for the design of two multibit models. One model was selected to achieve minimum insertion loss and low-power operation while the other was designed for optimum trade off between insertion loss and temperature stability.

The multibit models use the basic configuration shown in Fig. 1. Dielectric spacers separate adjacent toroids to reduce bit interaction. Locating the electronic driver circuits adjacent to the microwave portion of the device conserves space and driver energy requirements and reduces the charging current path length. The schematic of the driver used for the multibit models is shown in Fig. 7. The variable resistor allows electrical trimming of the peak pulse current on one side of the hysteresis loop, thus yielding an electrical trim of differential phase shift.

The low loss, low power model has five bits and uses an aluminum garnet with no rare earth substitutions for temperature compensation. The VSWR and insertion loss of this model is shown in Fig. 8. The figure of merit is approximately 570 degrees per dB across most of the frequency range. The phase slopes of the five bits are virtually zero.

The peak-power limiting threshold for the low-power model is one kilowatt. Because of the more narrow linewidth of the aluminum garnet used, the peak power threshold is proportionately lower than that of corresponding $4\pi M_s$ materials shown in Table I.

The temperature variation of phase shift of the low-loss model is given in Fig. 9. The phase stability of the bits is approximately 0.25 percent/°C. The phase shift is generally proportional to the variation of $4\pi M_s$ with temperature. However, since the level of $4\pi M_r$ associated with each bit will vary according to the driver

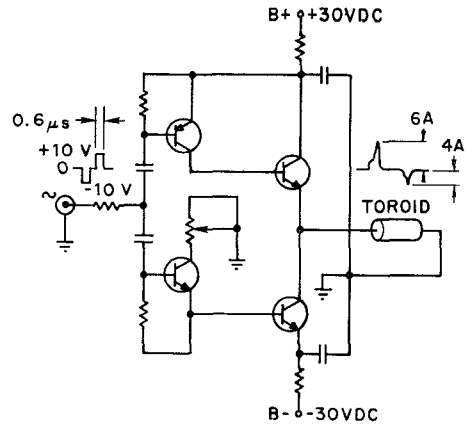

Fig. 7. Transistor driver circuit for latching toroids.

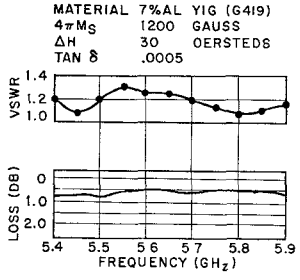

Fig. 8. VSWR and insertion loss of low power 5-bit model.

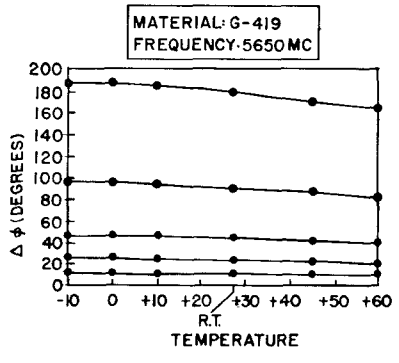

Fig. 9. Temperature variation in phase shift of low power model.

power, the exact differential phase shift vs. temperature characteristic will depend to a limited degree upon the electronic driver as well as the inherent material properties.

The variation in phase shift as shown in Fig. 9 may be excessive for some applications. This variation can be reduced with gadolinium doping of the garnet toroid materials. However, because of the resultant increase in loss due to the gadolinium, it is most desirable to elect a compromise between lowest loss and maximum temperature stability. Such a choice was made in the selection of Sperry G 484 material (8.5 percent aluminum-15 percent gadolinium doped YIG). The $4\pi M_s$ of this material was positioned at 900 gauss to enable 5 kW operation.

The VSWR and insertion loss of the G 484 four-bit

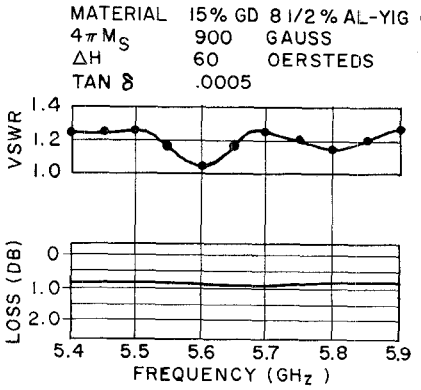

Fig. 10. VSWR and insertion loss for temperature compensated 4-bit model.

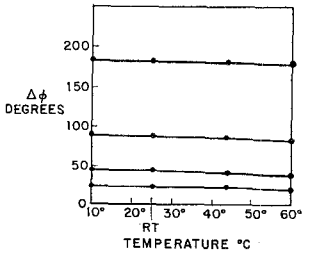

Fig. 11. Phase shift vs. temperature of temperature-stable model.

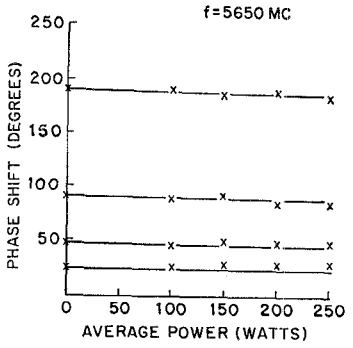

Fig. 12. Phase shift vs. average power for temperature compensated model.

model is shown in Fig. 10. The phase slope of each of the four bits is again essentially zero with frequency. The temperature stability of the differential phase shift is shown in Fig. 11 and represents an improvement by a factor of 2.5 over the low-power model. The peak-power limiting threshold of the device is 5.5 kilowatts.

Figure 12 shows the average power characteristics of the model using G 484 material and external air cooling. The phase stability with average power was approximately 0.021 percent/watt. It appears that successful operation up to 250 watts average can be achieved with external air cooling in the temperature compensated four-bit model.

Table II is a summary of the performance of the two multibit models and Fig. 13 depicts the packaged phase shifter with electronic drivers in final form.

TABLE II
SUMMARY OF THE PERFORMANCE OF TWO MULTIBIT MODELS

Performance Data Multibit Model		
	Low Power	High Power
No. Bits	5	4
Material	7% AL-YIG (G419)	15% GD-8.5% AL-YIG (G484)
VSWR	1.2 Nom	1.25 Nom
Loss	(dB) 0.6 Nom	(dB) 0.9 Nom
Phase Dev with Freq	<2%	<2%
Peak Power Threshold	1 kW	5.5 kW
Average PWR Rating	200 watts	250 watts
Phase Stability with Avg Power	0.023%/watt	0.021%/watt
Phase Stability with Temp	0.25%/°C	0.1%/°C
Length	10.156 in	11 in
Weight	8 oz	8.7 oz

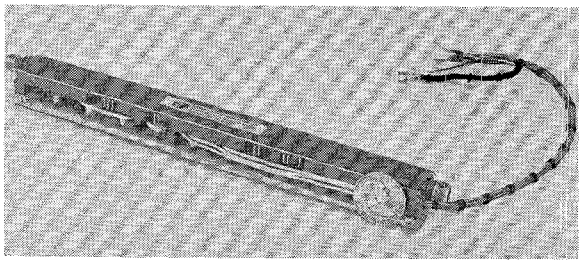

Fig. 13. Miniaturized C-band digital-latching phase shifter.

CONCLUSION

The measurements made on the devices described in this paper indicate that practical miniaturized light weight phase shifters are feasible for moderate power phased-array antenna application. In particular, the design is well suited to half-wavelength stacking of the phase shifters in an array.

The transition device is not limited to phase-shifter application or G-band frequencies and has been successfully applied to L and S band devices. The phase-shifter configuration could obviously be converted to waveguide input and output, if it should be more compatible with antenna requirements. The general approach appears to offer desirable antenna design and layout possibilities to the phased array systems engineer.

ACKNOWLEDGMENT

The authors express their appreciation to T. W. Sanders for his assistance in the laboratory, and to D. R. Taft and Dr. G. P. Rodrique for their many helpful suggestions.

References

[1] D. R. Taft et al., "Ferrite digital phase shifters," presented at the 1965 IEEE G-MTT Internat'l Symp., Clearwater, Fla.
[2] L. R. Whicker and R. R. Jones, "A digital latching ferrite strip transmission line phase shifter," *IRE Trans. on Microwave Theory and Techniques*, vol. MTT-13, pp. 781–784, November 1965.
[3] G. L. Heiter, "A latching type ferrite coaxial S-band phase shifter," *Proc. 1965 INTERMAG Conf.*, pp. 3.3–6.
[4] K. J. Button, "Theory of non-reciprocal ferrite phase shifters in dielectric-loaded coaxial line," *J. Appl. Phys.*, vol. 29, p. 998, 1958.
[5] P. H. Vartanian, Jr., et al., "Propagation in dielectric slab loaded rectangular waveguide," *IEEE Trans. on Microwave Theory and Techniques*, vol. MTT-6, pp. 215–222, April 1958.
[6] J. L. Allen, "The analysis of dielectrically loaded ferrite phase shifters including the effect of losses," Ph.D. dissertation, Georgia Inst. Tech., Atlanta, May 1966.
[7] W. J. Ince and E. Stern, "Computer analysis of ferrite digital phase shifters," *IEEE Internat'l Conv. Rec.*, pt. 5, 1966.
[8] D. R. Taft, private communication.
[9] D. R. Taft et al., "High power performance of ferrite digital phase shifters," presented at the 1966 NEREM Conf., Boston, Mass.

Correspondence

Microwaves at Japanese Universities

Introduction

The present status of the research in the fields of microwaves, millimeter waves, and coherent optical waves at Japanese universities is reviewed. A representative bibliography of over 90 references, which have appeared during the period of the last two years, including the papers to be published shortly, appears at the end of this summary. Among these, some selected topics are described herein briefly. Excluded are most of the works in microwave antennas and propagations, microwave tubes, and the physics of quantum electronics.

Like the recent trends in the United States and Europe, the current interest of the microwave researchers at Japanese universities is changing from the conventional microwave or millimeter wave transmission lines and components to the newly developed subjects such as leaky waveguides and beam waveguides, plasma electronics, quantum electronics, coherent electromagnetic optics, and related areas. This would be seen from the references listed which are divided into eleven subject categories.

I. Electromagnetic Wave Theory [1]–[10]

The leaky wave modes, and the surface waves in magnetoionic medium are studied mathematically. In connection with the future space communications technology, some basic problems, for instance, the electromagnetic radiation which would be produced by the oscillating electric dipole moving in free space with constant relativistic velocity, are analyzed [10]. It is shown that the energy density radiated from the moving dipole increases with velocity in the direction of motion and, conversely, it decreases in the opposite direction.

II. Waveguide Theory [11]–[17]

The waveguides containing inhomogeneous dielectrics [14], the slab of arbitrary admittance [13], and the waveguide filled with media composed of dielectrics and metallic blades [17] are treated. The expressions for the equivalent width of the waveguide composed of arbitrary wall impedances are derived [12], which may conveniently be used for the analysis of nonconventional waveguides such as striplines or trough waveguides.

A new family of "parabolic waveguide" whose cross section is formed by a pair of symmetric confocal parabolic conducting walls is proposed, and the interesting and promising features are shown theoretically [16].

III. Circular TE_{01} Waveguide [18]–[25]

The reflection and the mode conversion in multimode waveguide are discussed with emphasis on the resonance phenomena which would occur at, or in the immediate vicinity of, the cutoff frequencies of the modes involved [23]–[25].

An interesting novel method to prevent the mode conversion losses at a circular bend of the TE_{01} waveguide using inhomogeneous dielectrics and anisotropic wall impedance is proposed [20]. It is shown that the undesired coupling between the signal TE_{01} mode and both the unwanted TM_{11} and TE_{1n} modes due to the circular bend can be cancelled out all along the bend. This is accomplished by introducing a coupling of equal magnitude and opposite sign to that produced by the bend, by making an appropriate distribution of the permittivity across the cross section of the curved guide and an appropriate circumferential variation of the surface impedance of the guide wall. It is shown also that the appropriate slight deformation of the circular cross section of the curved guide provides just the same effect as that of an anisotropic wall impedance [19].

IV. Microwave Filters [26]–[29]

A design theory for the narrow band-pass harmonic resonator filters having extremely high midband frequency is developed, and is successfully confirmed by experiments at x-band [27]. A practical millimeter wave branching filter [29], three-path TEM-line higher harmonic rejection filter [26], and a utilization of the superconductivity for the low loss microwave filter [28] are studied.

V. Plasma Waveguides and Ferrite-Loaded Waveguides [30]–[35]

The electromagnetic fields in the ferrite-loaded cavities [30], [31] are analyzed theoretically in detail. The characteristics of the plasma-filled waveguides [33]–[35] and a parametric oscillation and amplification using YIG disk [32] are discussed.

VI. Open-Type Waveguides and Leaky Waveguides [36]–[46]

The beam waveguides, leaky waveguides, and surface waveguides, are being studied both from the theoretical interest and the interest of practical applications, especially to the high-speed-train control, train communications, and detection of obstacles on the railway track. The reflecting beam waveguides consisting of curved-strip conducting reflectors [36], and of cylindrical conducting reflectors [37] are analyzed theoretically.

VII. Microwave Measurements [47]–[52]

Synthesis of broadband matched load or absorbing wall is developed [48], [49]. A high sensitivity millimeter wave detection system is proposed [51]. The improved technique for measuring dielectric constants, [52] and the technique for precise measurement of the field distribution of surface waves [47] are also proposed.

VIII. Quasi-Optics and Optical Waveguides [53]–[60]

The wide-band quasi-optic dielectric prism components such as directional couplers, attenuators, and magic-tees using the Brewster angle matching technique are proposed [53], and are operated successfully at both millimeter [53] and optical [88] wavelengths. Because of the Brewster angle matching, the wave suffers no spurious reflections at the input and output boundary surfaces between air and dielectric, over a very large range of the frequencies affected only by the dispersion of the prism materials. Thus, directivity, broadbandness,

Manuscript received May 31, 1966.